JHEP

Published for SISSA by Springer

Received: January 2, 2020
Accepted: January 26, 2020
Published: February 26, 2020

Investigation of complex ϕ^4 theory at finite density in two dimensions using TRG

Daisuke Kadoh,[a,b] **Yoshinobu Kuramashi,**[c] **Yoshifumi Nakamura,**[d] **Ryo Sakai,**[e] **Shinji Takeda**[f] **and Yusuke Yoshimura**[c]

[a] *Physics Division, National Center for Theoretical Sciences, National Tsing-Hua University, Hsinchu, 30013, Taiwan*

[b] *Research and Educational Center for Natural Sciences, Keio University, Yokohama 223-8521, Japan*

[c] *Center for Computational Sciences, University of Tsukuba, Tsukuba 305-8577, Japan*

[d] *RIKEN Center for Computational Science, Kobe 650-0047, Japan*

[e] *Department of Physics and Astronomy, The University of Iowa, Iowa City, IA 52242, U.S.A.*

[f] *Institute for Theoretical Physics, Kanazawa University, Kanazawa 920-1192, Japan*

E-mail: kadoh@keio.jp, kuramasi@het.ph.tsukuba.ac.jp, nakamura@riken.jp, ryo-sakai@uiowa.edu, takeda@hep.s.kanazawa-u.ac.jp, yoshimur@ccs.tsukuba.ac.jp

Abstract: We study the two-dimensional complex ϕ^4 theory at finite chemical potential using the tensor renormalization group. This model exhibits the Silver Blaze phenomenon in which bulk observables are independent of the chemical potential below the critical point. Since it is expected to be a direct outcome of an imaginary part of the action, an approach free from the sign problem is needed. We study this model systematically changing the chemical potential in order to check the applicability of the tensor renormalization group to the model in which scalar fields are discretized by the Gaussian quadrature. The Silver Blaze phenomenon is successfully confirmed on the extremely large volume $V = 1024^2$ and the results are also ensured by another tensor network representation with a character expansion.

Keywords: Field Theories in Lower Dimensions, Lattice Quantum Field Theory

ArXiv ePrint: 1912.13092

https://doi.org/10.1007/JHEP02(2020)161

JHEP02(2020)161

Contents

1 Introduction

The tensor network (TN) is a promising approach to study lattice models with a sign problem. Coarse-graining algorithms of tensor networks such as the tensor renormalization group (TRG) [1] do not have any stochastic process unlike the Monte Carlo method which is based on the stochastic interpretation of the Boltzmann factor in path integrals. So a development of this approach could lead to deep understanding of quantum field theories that suffer from the sign problem such as QCD at finite chemical potential, finite θ angle, chiral gauge theories and SUSY theories. Although the TRG algorithm has been already introduced into the research of lattice quantum field theories [2–18], further studies are desirable to confirm if the TRG properly works for theories with a severe sign problem.

The complex ϕ^4 theory at finite chemical potential is the simplest model that suffers from a severe sign problem. This model exhibits the so-called Silver Blaze phenomenon in which bulk observables do not depend on the chemical potential below the critical point. Since it is directly related to the imaginary part of the action, various methods that could overcome the sign problem, such as the complex Langevin approach [19], the thimble method [20–22], and the worldline representation [23, 24], have been used to study the model. In case of TRG, it is not straightforward to apply the algorithm to the scalar field theory because the tensor indices are given by the field variable which takes any real or complex number and numerical computation is not directly applied to such an infinite dimensional tensor.

In refs. [15, 17] we have proposed a methodology of defining a finite dimensional tensor in the scalar field theory. We employed the Gaussian quadrature rule to discretize the scalar field so that a critical coupling constant of the Z_2 symmetry breaking in the two-dimensional real ϕ^4 theory is evaluated with the TRG procedure. The result was consistent with those obtained with other conventional methods. Namely, our discretization method effectively works for the real scalar field theory. This implies that the TRG approach with the discretized field variables can be also effective for a complex scalar field theory.

JHEP02(2020)161

In this paper, we study the two-dimensional complex ϕ^4 theory at finite chemical potential using the TRG method with the Gauss quadrature discretization for the scalar field. The expectation values for the scalar field and the number density are evaluated to investigate the Silver Blaze phenomenon. Furthermore, in order to confirm that the TRG method properly works, we compare the results to those obtained from another TN representation with the character expansion.

The rest of this paper is organized as follows: in section 2 we define the target model and construct the TN representation for the partition function. Numerical results are presented in section 3, where the Silver Blaze phenomenon is confirmed. We also make a comparison of the results obtained from the naive TN representation of the partition function and another TN representation. Section 4 is devoted to summary and future perspectives.

2 Two-dimensional complex ϕ^4 theory

The Euclidean continuum action of the two-dimensional complex ϕ^4 theory at finite chemical potential is defined by

$$S_{\text{cont}} = \int \mathrm{d}^2x \left\{ \sum_{\nu=1}^{2} |\partial_\nu \phi|^2 + \left(m^2 - \mu^2\right) |\phi|^2 + \mu \left(\phi^* \partial_2 \phi - \phi \partial_2 \phi^*\right) + \lambda |\phi|^4 \right\} \tag{2.1}$$

with a complex scalar field $\phi(x)$, the bare mass m, the quartic coupling constant $\lambda > 0$, and the chemical potential μ. This theory describes a relativistic Bose gas with finite chemical potential. The action is complex for $\mu \neq 0$ because the third term of eq. (2.1) is a pure imaginary number.

In the lattice theory, the scalar field denoted as ϕ_n lives on a site n of a lattice $\Gamma = \{(n_1, n_2) \,|\, n_\nu = 1, 2, \ldots, N_i\}$ with the lattice volume $V = N_1 \times N_2$. The lattice spacing a is set to 1. We assume that the scalar field satisfies the periodic boundary condition, $\phi_{n+N_\nu \hat{\nu}} = \phi_n$ for $\nu = 1, 2$, where $\hat{\nu}$ is the unit vector of the ν-direction. The lattice action is given by

$$S = \sum_{n \in \Gamma} \left[\left(4 + m^2\right) |\phi_n|^2 + \lambda |\phi_n|^4 - \sum_{\nu=1}^{2} \left(e^{\mu \delta_{\nu 2}} \phi_n^* \phi_{n+\hat{\nu}} + e^{-\mu \delta_{\nu 2}} \phi_n \phi_{n+\hat{\nu}}^* \right) \right]. \tag{2.2}$$

Note that the chemical potential is introduced as a pure imaginary constant vector potential in the temporal direction [25]. Since the lattice action also satisfies $(S(\mu))^* = S(-\mu)$, it is difficult to apply a naive Monte Carlo method to this model.

The partition function is defined as a standard manner:

$$Z = \int \mathcal{D}\phi \, e^{-S}, \tag{2.3}$$

where the complex field ϕ_n is represented in terms of two real fields as $\phi_n = \frac{1}{\sqrt{2}} (A_n + i B_n)$ and the integral measure is given by $\mathcal{D}\phi \equiv \prod_{n \in \Gamma} \mathrm{d}A_n \mathrm{d}B_n$. In the following we show that Z is represented as a tensor network according to refs. [15, 17]. The expectation value of any local field can also be represented as a tensor network in a similar way.

JHEP02(2020)161

The Boltzmann weight e^{-S} is expressed as a product of local factors:

$$e^{-S} = \prod_{n\in\Gamma} f_1\left(\phi_n, \phi_{n+\hat{1}}\right) f_2\left(\phi_n, \phi_{n+\hat{2}}\right), \tag{2.4}$$

where

$$f_\nu(w,z) = \exp\left\{-\left(1+\frac{m^2}{4}\right)\left(|w|^2+|z|^2\right) - \frac{\lambda}{4}\left(|w|^4+|z|^4\right) + e^{\mu\delta_{\nu 2}} w^* z + e^{-\mu\delta_{\nu 2}} w z^*\right\} \tag{2.5}$$

for $w, z \in \mathbb{C}$. It is possible to decompose the Boltzmann weight in this way as long as the lattice action contains only the nearest-neighbor interaction.

The continuous scalar field is discretized by the Gauss-Hermite quadrature rule to introduce a finite dimensional tensor as in refs. [15, 17]. For one-variable integration of a proper function $g(x)$, the quadrature provides a discretization as follows:

$$\int_{-\infty}^{\infty} \mathrm{d}x\, e^{-x^2} g\left(x\right) \approx \sum_{\alpha=1}^{K} w_\alpha g\left(y_\alpha\right) \tag{2.6}$$

where y_α and w_α are the α-th root of the K-th Hermite polynomial $H_K(x)$ and the corresponding weight defined as $w_\alpha = 2^{K-1}K!\sqrt{\pi}/(K^2 H_{K-1}(y_\alpha)^2)$, respectively. Here K dictates the order of approximation and for large K the accuracy of approximation is expected to be better.[1]

For the two-variable case ($\phi = \frac{1}{\sqrt{2}}(A+iB)$ with $A, B \in \mathbb{R}$), we have

$$\int_{-\infty}^{\infty} \mathrm{d}A \int_{-\infty}^{\infty} \mathrm{d}B\; e^{-2|\phi|^2} h\left(\phi\right) \approx \sum_{\alpha=1}^{K}\sum_{\beta=1}^{K} w_\alpha w_\beta\, h(\phi(\alpha,\beta)), \tag{2.7}$$

where

$$\phi(\alpha,\beta) \equiv \frac{y_\alpha + i y_\beta}{\sqrt{2}}. \tag{2.8}$$

Applying eq. (2.7) to each complex field, Z is approximated by $Z(K)$ as

$$Z \approx Z\left(K\right) = \sum_{\{\alpha,\beta\}} \prod_{n\in\Gamma} w_{\alpha_n} w_{\beta_n} \exp\left(y_{\alpha_n}^2 + y_{\beta_n}^2\right) \prod_{\nu=1}^{2} f_\nu\left(\phi(\alpha_n,\beta_n), \phi(\alpha_{n+\hat{\nu}}, \beta_{n+\hat{\nu}})\right), \tag{2.9}$$

where $\sum_{\{\alpha,\beta\}} \equiv \prod_{n\in\Gamma}\sum_{\alpha_n=1}^{K}\sum_{\beta_n=1}^{K}$.

As a result of the discretization, f_ν can be regarded as a $K^2 \times K^2$ complex valued matrix:

$$M^{[\nu]}_{\alpha\beta,\alpha'\beta'} \equiv f_\nu(\phi(\alpha,\beta), \phi(\alpha',\beta')) \tag{2.10}$$

[1] This depends on $g(x)$. In an actual computation, we check the convergence of result by increasing K.

JHEP02(2020)161

with the row index $\alpha, \beta = 1, 2, \ldots, K$ and the column index $\alpha', \beta' = 1, 2, \ldots, K$. Note that $\phi(\alpha, \beta)$ is given by discretized points y_α, y_β in eq. (2.8). Then the singular value decomposition is applied to the matrix:

$$M^{[\nu]}_{\alpha\beta,\alpha'\beta'} = \sum_{k=1}^{K^2} U^{[\nu]}_{\alpha\beta,k} \sigma^{[\nu]}_k V^{[\nu]\dagger}_{k,\alpha'\beta'}, \tag{2.11}$$

where $\sigma^{[\nu]}_k$ is k-th singular value sorted in the descending order, and $U^{[\nu]}$ and $V^{[\nu]}$ are $K^2 \times K^2$ unitary matrices with the row index α, β and the column index k. Plugging eq. (2.11) into eq. (2.9), we find that $Z(K)$ can be expressed as a tensor network,

$$Z(K) = \sum_{\{x,t\}} \prod_{n\in\Gamma} T_{x_n t_n x_{n-\hat{1}} t_{n-\hat{2}}}, \tag{2.12}$$

where

$$T_{ijkl} = \sqrt{\sigma^{[1]}_i \sigma^{[2]}_j \sigma^{[1]}_k \sigma^{[2]}_l} \sum_{\alpha,\beta=1}^{K} w_\alpha w_\beta \exp\left(y^2_\alpha + y^2_\beta\right) U^{[1]}_{\alpha\beta,i} U^{[2]}_{\alpha\beta,j} V^{[1]\dagger}_{k,\alpha\beta} V^{[2]\dagger}_{l,\alpha\beta} \tag{2.13}$$

and $\sum_{\{x,t\}} \equiv \prod_{n\in\Gamma} \sum_{x_n,t_n=1}^{K^2}$.

We obtain a finial expression by truncating the summation in eq. (2.12) up to D ($\leq K^2$) to reduce the computational complexity:

$$Z(K) \approx {\sum_{\{x,t\}}}' \prod_{n\in\Gamma} T_{x_n t_n x_{n-\hat{1}} t_{n-\hat{2}}}, \tag{2.14}$$

where ${\sum}'_{\{x,t\}} \equiv \prod_{n\in\Gamma} \sum_{x_n,t_n=1}^{D}$. This truncation keeps a better precision when $\sigma^{[\nu]}_k$ in eq. (2.11) has a sharp hierarchy structure. We should note that the initial tensor T depends on K. D becomes the bond dimension of tensors which is fixed throughout computations, and the convergence of results for K and D are checked numerically.

3 Numerical results

Numerical results of two-dimensional complex ϕ^4 theory at finite chemical potential are presented in this section. The TRG [1] is employed to coarse-grain the tensor network eq. (2.14) on a periodic lattice with the volume $V = N^2$ ($N = 2^m, m \in \mathbb{Z}$) and the lattice spacing $a = 1$. The coarse-graining procedure of partition function is briefly described in our previous paper [17] in which a procedure for the expectation value of a local field is also given. In the TRG algorithm, the SVD is truncated up to a fixed integer D, which is the bond dimension of tensors.

Figures 1 and 2 show the K-dependence and the D-dependence of the free energy density $f = -\frac{1}{V}\ln Z$ for a typical parameter set. K is the number of points used in the discretization of scalar fields as presented in eq. (2.7). The initial tensor eq. (2.13) depends on K since it is made of K-dependent unitary matrices associated with M in eq. (2.10). The result converges as both K and D increase, and $K = D = 64$, which are fixed in the following, are large enough to obtain converged results.

JHEP02(2020)161

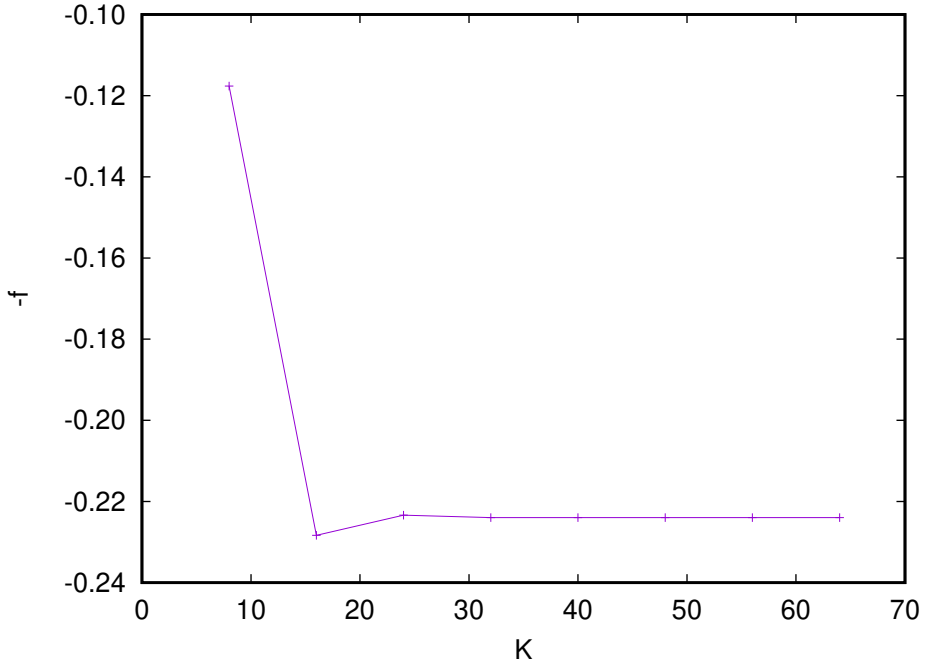

Figure 1. Free energy density for $D = 64$ and $m^2 = 0.01$, $\lambda = \mu = 1$ on $V = 1024^2$.

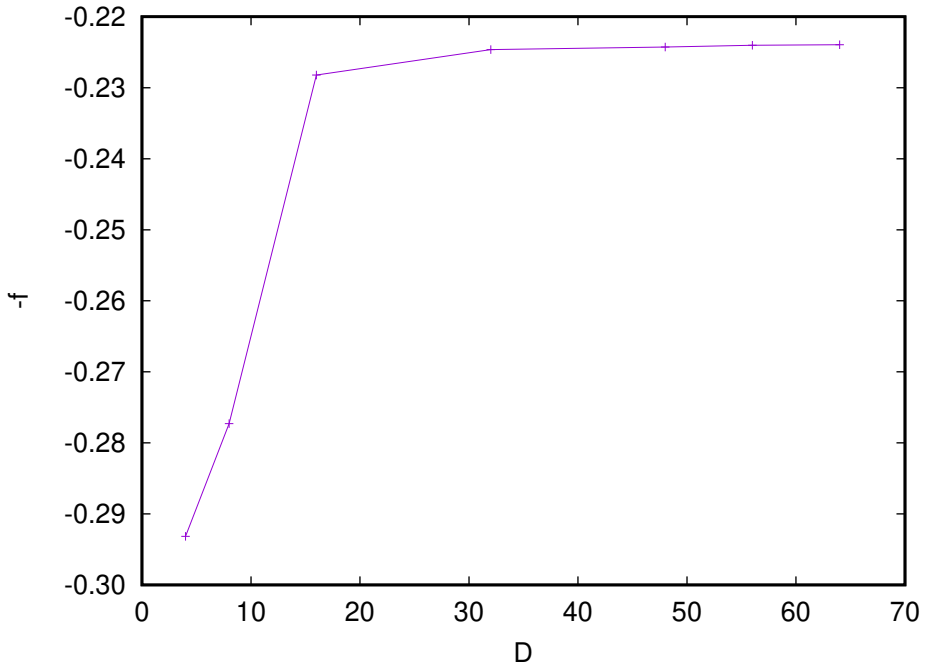

Figure 2. Free energy density for $K = 64$ and $m^2 = 0.01$, $\lambda = \mu = 1$ on $V = 1024^2$.

JHEP02(2020)161

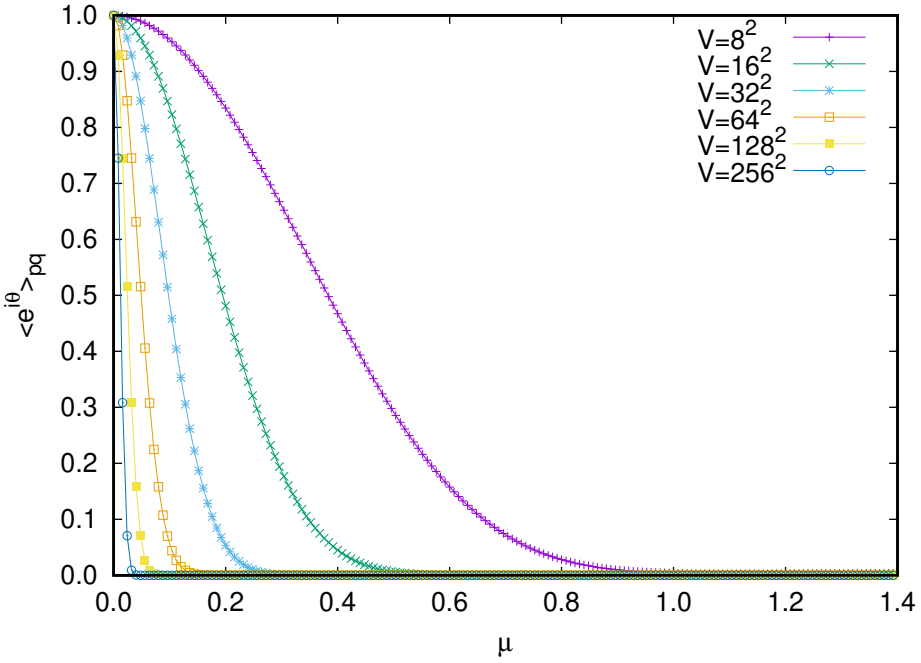

Figure 3. Average phase factor as a function of μ. The parameters are $m^2 = 0.01$, $\lambda = 1$, $K = D = 64$ and $V = 8^2, 16^2, \ldots, 256^2$. The sign problem becomes severe for larger μ and V.

3.1 Average phase factor

Let $\langle\cdot\rangle_{\rm pq}$ be an expectation value in the phase quenched theory with partition function,

$$Z_{\rm pq} = \int \mathcal{D}\phi\, e^{-{\rm Re}(S)}. \tag{3.1}$$

Then the expectation value of an operator $\mathcal{O}$ may be expressed as

$$\langle\mathcal{O}\rangle = \frac{\langle\mathcal{O}e^{i\theta}\rangle_{\rm pq}}{\langle e^{i\theta}\rangle_{\rm pq}}, \tag{3.2}$$

where $e^{-S} = e^{-{\rm Re}(S)}e^{i\theta}$. Using the TRG, $Z_{\rm pq}$ and $\langle\mathcal{O}\rangle_{\rm pq}$ for a local operator $\mathcal{O}$ can also be evaluated from a tensor dropping the last two terms in eq. (2.5).

The sign problem appears as a difficulty in evaluating the ratio of eq. (3.2). For large μ, since the phase factor $e^{i\theta}$ has a large fluctuation, both the average phase factor,

$$\langle e^{i\theta}\rangle_{\rm pq} = \frac{Z}{Z_{\rm pq}}, \tag{3.3}$$

and $\langle\mathcal{O}e^{i\theta}\rangle_{\rm pq}$ approach zero. Then, in the Monte Carlo method, it becomes difficult to evaluate $\langle\mathcal{O}\rangle$ due to a 0/0 problem. In other words, the severeness of the sign problem is measured by the numerical value of eq. (3.3).

Figure 3 shows the average phase factor evaluated by the TRG for various μ and V. We use $m^2 = 0.01$ and $\lambda = 1$ which are the same parameters as [24]. As clearly seen, the average phase factor decreases as μ increases for fixed space-time volume V while it also decreases as V increases for fixed μ. We thus confirm that, in the zero temperature and large spacial volume limits, severe sign problems happen even for small values of μ.

JHEP02(2020)161

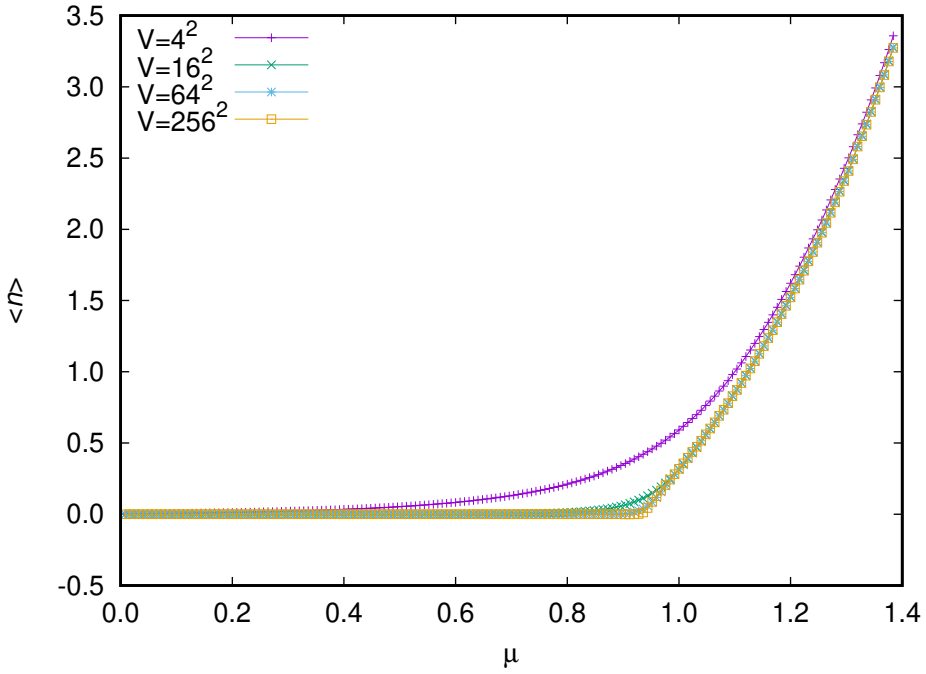

Figure 4. $\langle n \rangle$ as a function of μ. The lattice volume is varied from 4^2 to 256^2. The other parameters (m, λ, K and D) are the same as those of figure 3.

3.2 Silver Blaze phenomenon

In the thermodynamic limit, bulk observables are independent of μ below a critical μ_c as well as finite density QCD. This is called the Silver Blaze phenomenon which is a direct outcome of an imaginary part of the action. Although the computational cost of the Monte Carlo method has a large volume dependence, the TRG is suitable for observing the Silver Blaze phenomenon clearly since its cost scales with the logarithm of the lattice volume and the thermodynamic limit can be easily taken.

Figure 4 shows the μ-dependence of particle number density,

$$\langle n \rangle = \frac{1}{V} \frac{\partial \ln Z}{\partial \mu}. \tag{3.4}$$

The differentiation with respect to μ in the above equation is estimated by numerical differentiation. The Silver Blaze phenomenon is clearly observed for large volumes. The density does not depend on μ for small μ region, and it begins to increase at $\mu \approx 0.94$. In particular, the cusp structure around $\mu \approx 0.94$ tends to be sharper for larger volumes.

In figure 5, we compare the result of the number density to that of the phase quenched model on $V = 1024^2$. By contrast to the full theory, the phase quenched model exhibits the continuous behavior, and one can confirm that the μ independence of the result is a direct consequence of the imaginary part of the action. To see the difference in more detail, the volume dependence of the result at $\mu = 0.904$ is shown in figure 6. In the infinite volume limit, although the result in the full theory converges to zero, that in the phase quenched model converges to a non-zero value.

JHEP02(2020)161

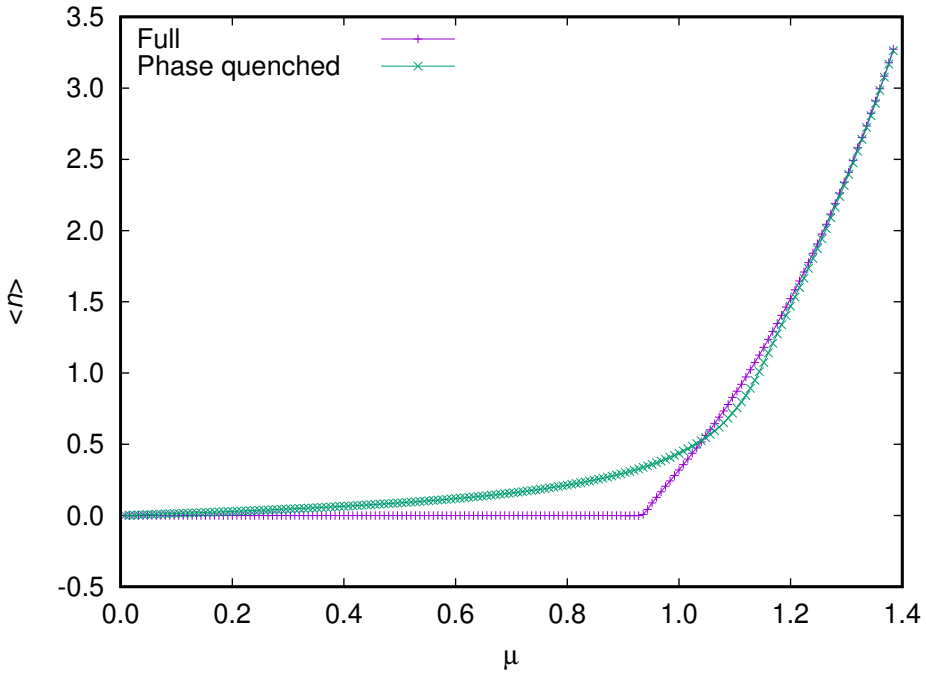

Figure 5. Comparison of the number density between the full and the phase quenched theories at $m^2 = 0.01$, $\lambda = 1$, $K = D = 64$ on $V = 1024^2$. The full theory clearly shows the Silver Blaze phenomenon unlike the phase quenched case.

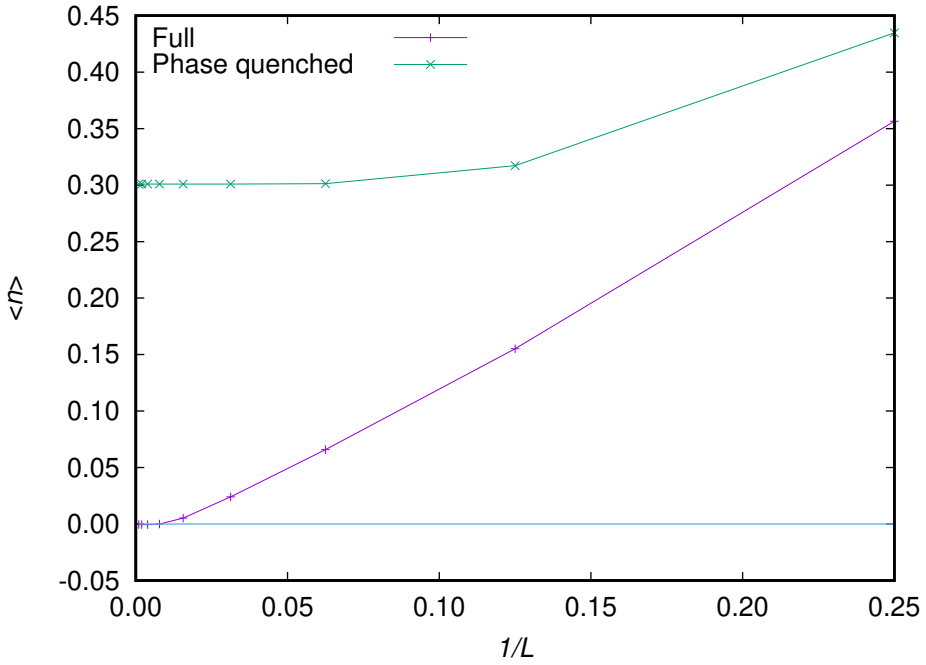

Figure 6. $\langle n \rangle$ as a function of $1/L$ at $\mu = 0.904$, $m^2 = 0.01$, $\lambda = 1$, $K = D = 64$. The density for the phase quenched case converges to a non-zero value while that for the full theory converges to zero in the thermodynamic limit.

JHEP02(2020)161

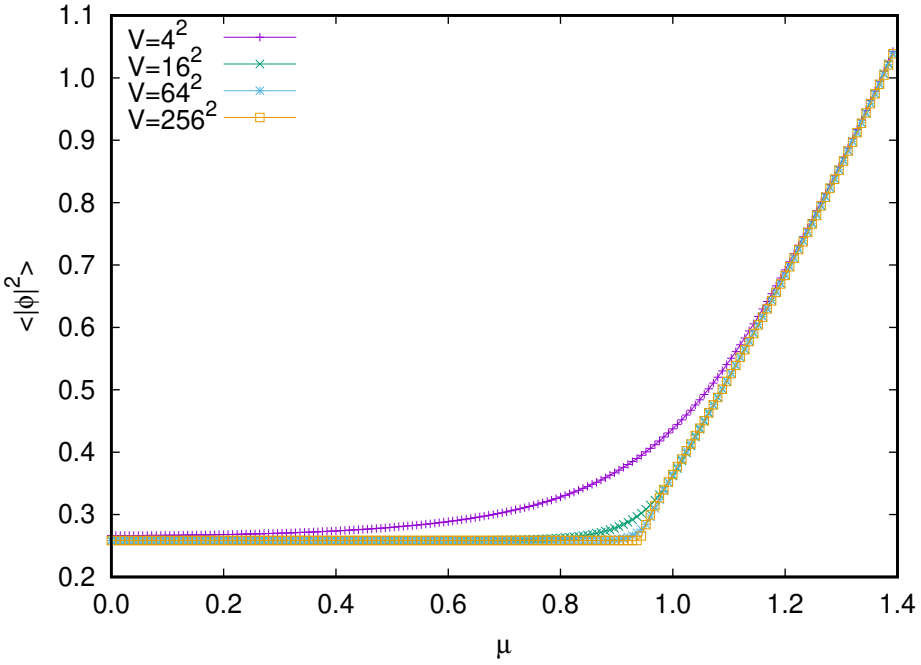

Figure 7. $\langle|\phi|^2\rangle$ as a function of μ. The other parameters (m, λ, K, D and V) are the same as those of figure 4.

Figure 7 shows $\langle|\phi|^2\rangle$ as a function of μ for the same parameters as those of figure 4, which is evaluated by the TRG with an impurity tensor [17]. As in the case of the density, the result is independent of μ for $\mu \lesssim 0.94$ and a sharp rise is seen around $\mu \approx 0.94$.

In order to study the stability of the Silver Blaze phenomenon against changing the physical parameters (m and λ), we also compute the particle number density for $(m^2, \lambda) = (0.01, 0.1)$ and $(0.1, 0.1)$ as shown in figure 8. Note that, for smaller m or λ, the exponential damping in the Boltzmann weight is weaker. Even for such cases, the Silver Blaze phenomenon is clearly observed.

3.3 Comparison with another tensor network representation

We have represented the partition function as a TN using the Gauss-Hermite quadrature for both the real and imaginary parts of each scalar field but one may use another representation, for instance, with a polar coordinate and the character expansion given in appendix A. It is known that the partition function in the case does not have an imaginary part. This formulation is also useful for the TN method. The Gaussian quadrature is needed only for the radial variable because the angular variable is transcribed into a tensor index with the character expansion. Thus, the cost of making the initial tensor is basically cheaper than making eq. (2.13). See appendix A for the details.

In figure 9, two representations are compared by showing $\langle|\phi|^2\rangle$ against μ. As a result they agree with each other well and it is hard to see the difference between them at this resolution. Thus we can conclude that choices of TN representation are basically irrelevant to our conclusion.

JHEP02(2020)161

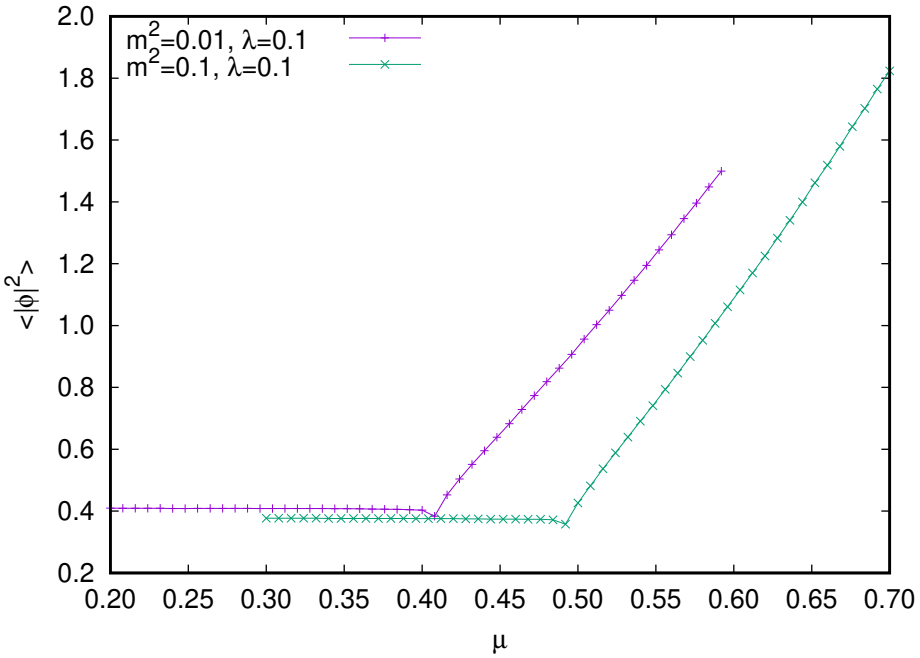

Figure 8. $\langle|\phi|^2\rangle$ as a function of μ at $K = 64$ and $D = 64$ on $V = 1024^2$. The Silver Blaze phenomenon is observed irrespective of the values of the physical parameters.

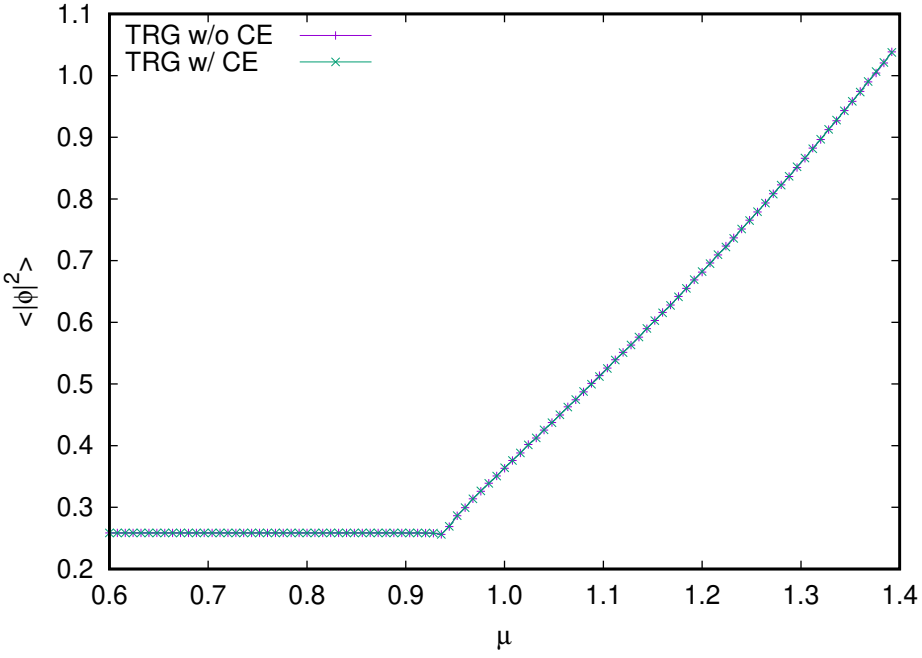

Figure 9. Comparison of $\langle|\phi|^2\rangle$ obtained by two different TN formulations with $D = 64$ on $V = 1024^2$. We use $K = 64$ for the first representation without the character expansion and $N_{CE} = 128$ and $K = 256$ for the second one with the character expansion. See the appendix for the details.

JHEP02(2020)161

4 Summary

In this paper we have derived a TN representation for the complex scalar field theory discretizing the continuous scalar fields with the Gauss-Hermite quadrature rule. Using the TRG procedure for the TN representation of partition function, the average phase factor, the particle number density and $\langle|\phi|^2\rangle$ were evaluated.

As a result, the Silver Blaze phenomenon is clearly observed for the extremely large volume $V = 1024^2$ which is essentially in the zero temperature and the large spacial volume limits. We also examine another TN representation using the character expansion. Then, our numerical results of two representations do not have a visible difference, and the conclusion does not change for the other TN representation. Thus we confirm that the TN method is effective for a quantum field theory with the severe sign problem.

Acknowledgments

We would like to thank Yoshimasa Hidaka and Akira Ohnishi for their helpful comments. This work was supported by the Ministry of Education, Culture, Sports, Science and Technology (MEXT) as "Exploratory Challenge on Post-K computer" (Frontiers of Basic Science: Challenging the Limits), the U.S. Department of Energy (DOE) under Award Number DE-SC0019139, and JSPS KAKENHI Grant Numbers JP17K05411, JP18J10663, and JP19K03853.

A Tensor network representation with a character expansion

In this appendix, an alternative TN representation of partition function is derived by a character expansion (see [26]).[2] To this end, the polar coordinate $\phi_n = r_n e^{i\theta_n}$ is helpful in using the character expansion of $e^{x\cos z}$:

$$e^{x\cos z} = \sum_{p=-\infty}^{\infty} I_p(x)\, e^{ipz} \qquad \text{for } x \in \mathbb{R},\ z \in \mathbb{C}, \tag{A.1}$$

where I_p is the p-th modified Bessel function of the first kind. In the polar coordinate, the lattice action eq. (2.2) is written as

$$S = \sum_{n\in\Gamma}\left[\left(4+m^2\right) r_n^2 + \lambda r_n^4 - 2\sum_{\nu=1}^{2}\cos(\theta_{n+\hat{\nu}} - \theta_n - i\mu\delta_{\nu 2}) r_n r_{n+\hat{\nu}}\right]. \tag{A.2}$$

Using the above formulas, a dual formulation of the partition function is obtained as

$$\begin{aligned} Z = &\left(\prod_{n\in\Gamma}\sum_{p_n,q_n=-\infty}^{\infty} 2\pi\int_0^\infty \mathrm{d}r_n r_n\, e^{-\left(4+m^2\right)r_n^2-\lambda r_n^4}\right) \\ &\times\prod_{n\in\Gamma} I_{p_n}(2r_n r_{n+\hat{1}}) I_{q_n}(2r_n r_{n+\hat{2}})\,\delta_{(p_n+q_n-p_{n-\hat{1}}-q_{n-\hat{2}}),0}\, e^{\mu q_n}. \end{aligned} \tag{A.3}$$

[2] If the Taylor expansion of the hopping term is used instead of the character expansion, another dual formulation is obtained [24].

JHEP02(2020)161

Integrating the angular variables turns out to be constraints for p and q variables with Kronecker's delta. Note that all entries of (A.3) are real and non-negative.

To define a finite dimensional tensor, we truncate the summation for p_n, q_n and discretize the radial variable r_n with Gauss-Hermite quadrature. In this case, since $r_n \in [0, \infty)$, we use the $2K$-point Gauss-Hermite quadrature with only the positive K nodes.[3] Then the discrete version of (A.3) is given by

$$Z\left(N_{\mathrm{CE}}, K\right) = \left(\prod_{n\in\Gamma} \sum_{p_n,q_n=-N_{\mathrm{CE}}}^{N_{\mathrm{CE}}} \sum_{\alpha_n=1}^{K}\right) \prod_{n\in\Gamma} 4\pi y_{\alpha_n} w_{\alpha_n} e^{y_\alpha^2} \times h_{p_n}(y_{\alpha_n}, y_{\alpha_{n+\hat{1}}}) h_{q_n}(y_{\alpha_n}, y_{\alpha_{n+\hat{2}}})\, \delta_{(p_n+q_n-p_{n-\hat{1}}-q_{n-\hat{2}}),0}\, e^{\mu q_n}, \tag{A.4}$$

where

$$h_p\left(r, s\right) = e^{-\left(1+\frac{m^2}{4}\right)\left(r^2+s^2\right)-\frac{\lambda}{4}\left(r^4+s^4\right)} I_p\left(2rs\right), \tag{A.5}$$

y_α is the αth positive root of $2K$ Gauss-Hermite polynomial, and w_α is the corresponding weight given by $w_\alpha \equiv 2^{2K-1}(2K)!\sqrt{\pi}/((2K)^2 H_{2K-1}(y_\alpha)^2)$. We have restricted the range of the summation of the character expansion to $[-N_{\mathrm{CE}}, N_{\mathrm{CE}}]$. The local Boltzmann factor $h_p(y_\alpha, y_\beta)$ with fixed p is now regarded as a $K \times K$ matrix to which the SVD can be applied:

$$h_p\left(y_\alpha, y_\beta\right) = \sum_{x=1}^{K} U_{\alpha x}^{[p]} \sigma_x^{[p]} V_{x\beta}^{[p]\dagger}. \tag{A.6}$$

Plugging eq. (A.6) into eq. (A.4) leads to a TN representation of $Z\left(N_{\mathrm{CE}}, K\right)$:

$$Z\left(N_{\mathrm{CE}}, K\right) = \left(\prod_{n\in\Gamma} \sum_{p_n,q_n=-N_{\mathrm{CE}}}^{N_{\mathrm{CE}}} \sum_{x_n,t_n=1}^{K}\right) \prod_{n\in\Gamma} \tilde{T}^{p_n q_n p_{n-\hat{1}} q_{n-\hat{2}}}_{x_n t_n x_{n-\hat{1}} t_{n-\hat{2}}}, \tag{A.7}$$

where

$$\tilde{T}^{abcd}_{ijkl} = 4\pi \sqrt{\sigma_i^{[a]} \sigma_j^{[b]} \sigma_k^{[c]} \sigma_l^{[d]}}\, e^{\mu b}\, \delta_{a+b,c+d} \sum_{\alpha=1}^{K} y_\alpha w_\alpha e^{y_\alpha^2} U_{\alpha i}^{[a]} U_{\alpha j}^{[b]} V_{k\alpha}^{[c]\dagger} V_{l\alpha}^{[d]\dagger}. \tag{A.8}$$

Note that $(x_n, p_n), (t_n, q_n), (x_{n-\hat{1}}, p_{n-\hat{1}}), (t_{n-\hat{2}}, q_{n-\hat{2}})$ may be interpreted as four index pairs defined on four different links stemmed from the site n. Thus $\tilde{T}$ may be interpreted as a rank-4 tensor whose bond dimension is $K \times (2N_{\mathrm{CE}} + 1)$ since $x_n, t_n = 1, 2 \ldots, K$ and $p_n, q_n = -N_{\mathrm{CE}}, \ldots, N_{\mathrm{CE}}$.

In an actual computation, the summations $\sum_{p_n=-N_{\mathrm{CE}}}^{N_{\mathrm{CE}}} \sum_{x_n=1}^{K}$ (and $\sum_{q_n=-N_{\mathrm{CE}}}^{N_{\mathrm{CE}}} \sum_{t_n=1}^{K}$) in eq. (A.7) are reduced by including D largest singular values $\sigma_x^{[p]}$ of eq. (A.8) into the computation. Let us arrange $\sigma_x^{[p]}$ in the descending order for all x and p and suppose that the nth largest singular value is $\sigma_{x'}^{[p']}$. Then a one-to-one mapping f between n and (x', p')

[3] One can of course use other quadrature rules such as the Gauss-Legendre or the Gauss-Laguerre. With sufficiently large number of Gaussian nodes, the detail of the quadrature rule does not matter to the accuracy.

JHEP02(2020)161

can be given, that is, $n = f(x', p')$.[4] Using this mapping, the combined index X_n and T_n are given by

$$X_n = f(x_n, p_n), \quad T_n = f(t_n, q_n). \tag{A.9}$$

Once f is given, X_n is uniquely given for x_n, p_n and vice versa. Then the tensor is represented as

$$T^{(\mathrm{CE})}_{XTX'T'} \equiv \tilde{T}^{pqp'q'}_{xtx't'}, \tag{A.10}$$

with $(x, p) = f^{-1}(X), (t, q) = f^{-1}(T)$ and the same identifications for X', T'. Then truncated version of the discretized partition function is given by

$$Z\left(N_{\mathrm{CE}}, K\right) \approx \left(\prod_{n \in \Gamma} \sum_{X_n, T_n = 1}^{D} \right) \prod_{n \in \Gamma} T^{(\mathrm{CE})}_{X_n T_n X_{n-\hat{1}} T_{n-\hat{2}}}. \tag{A.11}$$

For a given D and K, the mapping f is uniquely determined up to D (except for an issue of degenerate singular values) because it is stable in practice when N_{CE} is varied in a range of sufficiently large values. So $T^{(\mathrm{CE})}$ does not depend on N_{CE}, but only on K. In this sense, the N_{CE}-dependence of $Z\left(N_{\mathrm{CE}}, K\right)$ is small and is not observed as long as it is approximated by r.h.s. of eq. (A.11).

References

[1] M. Levin and C.P. Nave, *Tensor renormalization group approach to 2D classical lattice models*, *Phys. Rev. Lett.* **99** (2007) 120601 [cond-mat/0611687] [INSPIRE].

[2] Y. Shimizu, *Analysis of the* $(1+1)$*-Dimensional Lattice* ϕ^4 *Model Using the Tensor Renormalization Group*, *Chin. J. Phys.* **50** (2012) 749.

[3] Y. Liu et al., *Exact Blocking Formulas for Spin and Gauge Models*, *Phys. Rev.* **D 88** (2013) 056005 [arXiv:1307.6543] [INSPIRE].

[4] J.F. Yu et al., *Tensor Renormalization Group Study of Classical XY Model on the Square Lattice*, *Phys. Rev.* **E 89** (2014) 013308 [arXiv:1309.4963] [INSPIRE].

[5] A. Denbleyker et al., *Controlling Sign Problems in Spin Models Using Tensor Renormalization*, *Phys. Rev.* **D 89** (2014) 016008 [arXiv:1309.6623] [INSPIRE].

[6] Y. Shimizu and Y. Kuramashi, *Grassmann tensor renormalization group approach to one-flavor lattice Schwinger model*, *Phys. Rev.* **D 90** (2014) 014508 [arXiv:1403.0642] [INSPIRE].

[7] J.F. Unmuth-Yockey, Y. Meurice, J. Osborn and H. Zou, *Tensor renormalization group study of the* 2*d* $O(3)$ *model*, PoS(LATTICE2014)325 (2014) [arXiv:1411.4213] [INSPIRE].

[4] For degenerate singular values, one may give the mapping in arbitrary order.

JHEP02(2020)161

[8] Y. Shimizu and Y. Kuramashi, *Critical behavior of the lattice Schwinger model with a topological term at $\theta = \pi$ using the Grassmann tensor renormalization group*, *Phys. Rev.* **D 90** (2014) 074503 [arXiv:1408.0897] [INSPIRE].

[9] S. Takeda and Y. Yoshimura, *Grassmann tensor renormalization group for the one-flavor lattice Gross-Neveu model with finite chemical potential*, *PTEP* **2015** (2015) 043B01 [arXiv:1412.7855] [INSPIRE].

[10] H. Kawauchi and S. Takeda, *Tensor renormalization group analysis of $CP(N-1)$ model*, *Phys. Rev.* **D 93** (2016) 114503 [arXiv:1603.09455] [INSPIRE].

[11] Y. Meurice, A. Bazavov, S.-W. Tsai, J. Unmuth-Yockey, L.-P. Yang and J. Zhang, *Tensor RG calculations and quantum simulations near criticality*, PoS(LATTICE2016)325 (2016) [arXiv:1611.08711] [INSPIRE].

[12] R. Sakai, S. Takeda and Y. Yoshimura, *Higher order tensor renormalization group for relativistic fermion systems*, *PTEP* **2017** (2017) 063B07 [arXiv:1705.07764] [INSPIRE].

[13] Y. Yoshimura, Y. Kuramashi, Y. Nakamura, S. Takeda and R. Sakai, *Calculation of fermionic Green functions with Grassmann higher-order tensor renormalization group*, *Phys. Rev.* **D 97** (2018) 054511 [arXiv:1711.08121] [INSPIRE].

[14] Y. Shimizu and Y. Kuramashi, *Berezinskii-Kosterlitz-Thouless transition in lattice Schwinger model with one flavor of Wilson fermion*, *Phys. Rev.* **D 97** (2018) 034502 [arXiv:1712.07808] [INSPIRE].

[15] D. Kadoh, Y. Kuramashi, Y. Nakamura, R. Sakai, S. Takeda and Y. Yoshimura, *Tensor network formulation for two-dimensional lattice $\mathcal{N} = 1$ Wess-Zumino model*, *JHEP* **03** (2018) 141 [arXiv:1801.04183] [INSPIRE].

[16] Y. Kuramashi and Y. Yoshimura, *Three-dimensional finite temperature Z_2 gauge theory with tensor network scheme*, *JHEP* **08** (2019) 023 [arXiv:1808.08025] [INSPIRE].

[17] D. Kadoh, Y. Kuramashi, Y. Nakamura, R. Sakai, S. Takeda and Y. Yoshimura, *Tensor network analysis of critical coupling in two dimensional ϕ^4 theory*, *JHEP* **05** (2019) 184 [arXiv:1811.12376] [INSPIRE].

[18] Y. Kuramashi and Y. Yoshimura, *Tensor renormalization group study of two-dimensional U(1) lattice gauge theory with a θ term*, arXiv:1911.06480 [INSPIRE].

[19] G. Aarts, *Can stochastic quantization evade the sign problem? The relativistic Bose gas at finite chemical potential*, *Phys. Rev. Lett.* **102** (2009) 131601 [arXiv:0810.2089] [INSPIRE].

[20] M. Cristoforetti, F. Di Renzo, A. Mukherjee and L. Scorzato, *Monte Carlo simulations on the Lefschetz thimble: Taming the sign problem*, *Phys. Rev.* **D 88** (2013) 051501 [arXiv:1303.7204] [INSPIRE].

[21] H. Fujii, D. Honda, M. Kato, Y. Kikukawa, S. Komatsu and T. Sano, *Hybrid Monte Carlo on Lefschetz thimbles — A study of the residual sign problem*, *JHEP* **10** (2013) 147 [arXiv:1309.4371] [INSPIRE].

[22] Y. Mori, K. Kashiwa and A. Ohnishi, *Application of a neural network to the sign problem via the path optimization method*, *PTEP* **2018** (2018) 023B04 [arXiv:1709.03208] [INSPIRE].

[23] C. Gattringer and T. Kloiber, *Lattice study of the Silver Blaze phenomenon for a charged scalar ϕ^4 field*, *Nucl. Phys.* **B 869** (2013) 56 [arXiv:1206.2954] [INSPIRE].

JHEP02(2020)161

[24] O. Orasch and C. Gattringer, *Canonical simulations with worldlines: An exploratory study in ϕ^4_2 lattice field theory*, *Int. J. Mod. Phys.* **A 33** (2018) 1850010 [arXiv:1708.02817] [INSPIRE].

[25] P. Hasenfratz and F. Karsch, *Chemical Potential on the Lattice*, *Phys. Lett.* **125B** (1983) 308 [INSPIRE].

[26] M.G. Endres, *Method for simulating O(N) lattice models at finite density*, *Phys. Rev.* **D 75** (2007) 065012 [hep-lat/0610029] [INSPIRE].

JHEP02(2020)161